J Am Oil Chem Soc (2011) 88:1113–1123
DOI 10.1007/s11746-011-1769-0

ORIGINAL PAPER

Crystallization and Polymorphism of 1,3-Acyl-Palmitoyl-*rac*-Glycerols

R. John Craven · Robert W. Lencki

Received: 2 September 2010 / Revised: 8 December 2010 / Accepted: 17 January 2011 / Published online: 18 February 2011

Abstract Crystallization and melting behavior, small-angle X-ray scattering, X-ray powder diffraction and infra-red absorbance were measured for nine 1,3-acyl-palmitoyl-*rac*-glycerols (1,3-acetoyl-, -butyroyl-, -hexanoyl-, -octanoyl-, -decanoyl-, -lauroyl, -myristoyl- and -oleoyl-palmitoyl-*rac*-glycerol and 1,3-dipalmitoyl-glycerol). All but one of the prepared 1,3-diacylglycerols (1,3-DAG) were β-stable with 1,3-acetoyl-palmitoyl-*rac*-glycerol being the exception (β'-stable). Small-angle X-ray scattering indicates that molecules in β-tending diacid 1,3-DAG adopt a herringbone-type configuration similar to monoacid 1,3-DAG. In this configuration acyl chains of the same length associate and regular chain-end matching between terminal methyl groups delineate lamellae. In contrast, molecules in crystalline 1,3-acetoyl-palmitoyl-*rac*-glycerol are oriented similar to those of 1(3)-monoacylglycerol. Interestingly, DSC curves indicate five of the nine diacid compounds have meta-stable forms—suggesting these forms are quite common for diacid 1,3-DAG. Meta-stable forms are observed in the melting curve when the difference in length between acyl chains is large (1,3-acetoyl-, -butyroyl- and -hexanoyl-palmitoyl-*rac*-glycerol), and in the crystallization curve when the difference is moderate (1,3-decanoyl- and -lauroyl-palmitoyl-*rac*-glycerol).

Keywords 1,3-Diacylglycerol · Physical chemistry · X-ray powder diffraction · Small-angle X-ray scattering · Infra-red spectroscopy · Polymorphism

R. J. Craven · R. W. Lencki (✉)
Department of Food Science, University of Guelph, Guelph, ON N1G 2W1, Canada
e-mail: rlencki@uoguelph.ca

Introduction

1,3-Diacylglycerol (1,3-DAG) play a key role in a number of industrially important systems. For example, they are components of natural fats and oils (e.g. palm oil, milk fat) and are known to influence their nucleation, crystal growth and polymorphism [1–4]. DAG are also used as food emulsifiers and as intermediates in the preparation of specific structured lipids and pharmaceutical products [5]. In addition, replacing dietary TAG with 1,3-DAG reportedly leads to weight loss and improves blood cholesterol levels due to a difference in the way the molecules are metabolized [6]. To further develop 1,3-DAG-based products for these applications, a detailed understanding of their physical characteristics is required.

The phase behavior of DAG is quite complex and therefore of particular interest. While 1,2-diacylglycerols crystallize in α and β' polymorphs, the majority of 1,3-DAG are β-tending—crystallizing in either high-melting β_1 or low-melting β_2 forms [7]. There are however exceptions; for example, diacid 1,3-DAG containing both short- and long-chain acyl groups (e.g. 1,3-acetoyl-stearoyl-*rac*-glycerol) are reportedly β'-tending [8].

The complete melting behavior for monoacid 1,3-DAG of long-chain FA (viz. 1,3-dipalmitin and 1,3-distearin) has been determined [9] and the melting points (β_1 and β_2 forms) of many other monoacid 1,3-DAG have been reported [10]. In addition, the conformation of the most stable form for 1,3-dilaurin has been ascertained by single-crystal X-ray studies [11, 12]. By comparison, diacid 1,3-DAG have received far less attention—perhaps because they are not commercially available and are a challenge to prepare. In general, only polymorphic tendency (β- or β'-tending) and melting point of the highest-melting form have been reported for diacid 1,3-DAG [10].

Even for the most remarkable of these molecules (e.g. 1,3-acetoyl-palmitoyl-*rac*-glycerol), which display exceptional polymorphism (β'-tending), complete crystallization and melting behavior has yet to be analyzed by DSC—although it has been studied by dilatometry [8]. This is not surprising since most of the published data was collected in the 1940s and 1950s, prior to the first commercial DSC (1964). Likewise, literature values are questionable because, at the time, methodologies for determining purity of starting materials and final products were not fully developed [13].

Thus, the first goal of this work was to characterize 1,3-acyl-palmitoyl-*rac*-glycerols using current, consistent and recognized methods. To this end, X-ray powder diffraction (XRD), small-angle X-ray scattering (SAXS), infra-red spectroscopy (IR) and differential scanning calorimetry (DSC) were used to examine 1,3-acyl-palmitoyl-*rac*-glycerols (acetoyl-, butyroyl-, hexanoyl-, octanoyl-, decanoyl-, lauroyl-, myristoyl- and oleoyl-palmitoyl-*rac*-glycerol and 1,3-dipalmitoyl-glycerol). After placing this new data in context (by comparing with existing literature), the role of acyl chain length in the crystallization behavior of 1,3-acyl-palmitoyl-*rac*-glycerols could be examined by comparing results for compounds within the series.

Materials and Methods

Unless noted otherwise, reagents, chemicals and enzymes were purchased from Sigma-Aldrich (Mississauga, ON, Canada) and were of the highest practical grade; solvents were purchased from Fisher Scientific (Ottawa, ON, Canada) and were HPLC grade. The declared purity of free fatty acids (FFA) was: hexanoic (6:0) and myristic (14:0) acids $\approx$99.5%, palmitic (16:0) acid $\geq$96%, lauric (12:0) acid $\geq$95% and oleic (18:1) acid $\geq$90% purity. The declared purity of acid chlorides was: butyroyl (4:0) and octanoyl (8:0) chloride $\geq$99%, decanoyl (10:0), lauroyl and palmitoyl chloride $\approx$98% and hexanoyl chloride $\approx$97% purity. Solketal (isopropylidene glycerol) and acetic anhydride were both 98% purity. The vinyl ester of palmitic acid donated by Japan Vam & Poval (Osaka, Japan) was $\geq$96% purity.

Synthesis

Diacid 1,3-DAG were prepared by reacting 1(3)-MAG with acid chlorides and triethylamine in the presence of 4-dimethylaminopyridine [14, 15]. Monoacid 1,3-DAG were prepared by mixing glycerol with a fatty acid vinyl ester in the presence of immobilized lipase B from *Candida antarctica* [16]. 1(3)-MAG precursors were synthesized following published methods [17, 18] with the following exceptions: solketal was used as a starting material; shorter reflux times ($\sim$5 h) were employed; and free 1(3)-MAG was produced using an acidic cation exchange resin [19]. The resulting MAG and DAG were purified by recrystallization or flash chromatography.

Gas Chromatography

Trimethylsilyl-derivatives were analyzed on a 25 m $\times$ 0.25 mm polarizable capillary column (Quadrex, Woodbridge, CT, USA) [15]. The column was housed in a Hewlett Packard 5890 (Agilent, Palo Alto, CA, USA) GC equipped with FID and on-column inlet. The inlet pressure for the carrier gas (hydrogen) was set to 15 psi, cool on-column injection was employed and the detector was held at 370 °C. After sample injection, the oven was held at 60 °C for 2 min, then the temperature was increased to 250 °C at 35 °C/min, and finally the temperature was increased to 300 °C at 4 °C/min.

Differential Scanning Calorimetry

Crystallization and melting curves were determined using a Q1000 DSC (TA Instruments, New Castle, DE, USA) that was calibrated following the manufacturer's recommendations with a pure indium standard and a matched pair of sapphires. The sample cell was purged with dry nitrogen flowing at 25 mL/min. Hermetically sealed alodined aluminum DSC pans containing 4–8 mg of the sample were processed and heat flow was measured relative to an empty sealed DSC pan. Results were analyzed using Universal Analysis software version 4.2E (TA instruments).

Samples were prepared by transferring solid DAG to the sample pan without melting; the initial melt of these samples was measured (at 5 °C/min). This provided the melting data (T_e, T_p and ΔH_f) for the high-melting form of each compound. Afterwards, samples were analyzed by DSC at three different heating/cooling rates (2.5, 5 and 10 °C/min) because DSC scans collected at several rates are useful for detecting polymorphism [20]. Universal Analysis software was used to determine the extrapolated onset temperature (T_e), peak temperature (T_p) and enthalpy (ΔH_f) of both melting and crystallization. Measurements obtained from melting curves are considered more reliable than those arising from crystallization because the latter requires undercooling and is delayed by the need for nucleation [21]. The preferred measurement of melting temperature (T_m) is the extrapolated onset of melting temperature (T_e) because it has been shown to vary the least with heating rate. T_e is the temperature at which a tangent through the linear portion of the leading edge of the peak intersects with the baseline [22]. In the event that T_e is not available, as is the case with peaks

that merge due to polymorphism, T_p is an acceptable approximation [21, 22].

Infra-Red Spectroscopy

Data was collected using a Shimadzu IRPrestige-12 FTIR (Kyoto) equipped with a Pike MIRacle™ ATR sample stage (Madison, WI, USA). Data was analyzed using the Shimadzu IR Solution 1.30 software package.

X-Ray Powder Diffraction

Solid samples were ground into fine powders and applied to sample slides with a 0.2 mm deep depression (Rigaku, Tokyo Japan). An aftermarket temperature controller utilizing Peltier cooling (Electron Dynamics, Southampton, UK) maintained the sample stage at 20 °C. Powder diffraction data was recorded using a Rigaku Multiflex powder X-ray diffractometer with a CuK_α radiation ($\lambda = 1.5406$ Å [23]) and a scintillation detector. Samples were scanned from 2 to 30 degrees at 2 degrees/min. Results were analyzed and major peaks were identified using Jade software version 6.5 (Materials Data, Livermore, CA, USA).

Small Angle X-Ray Scattering

Samples were ground into a fine powder and sealed between sheets of Kapton. Samples were held at 20 °C in a temperature-controlled stage while data was recorded using a Nanostar SAXS (Bruker AXS, Madison, WI, USA) with CuK_α radiation and a High Star wire-type detector. Results were analyzed using Bruker AXS software version 4.1.26.

Table 1 DSC melting data for 1,3-acyl-palmitoyl-*rac*-glycerols

FA		T_e (°C)	T_p (°C)	ΔH_f (kJ/mol)	Literature (°C)	
2:0	β'	25.33	31.55	–	43.6[a]	41.0[b]
		9.90	29.58	–	35.0[a]	33.5[b]
4:0	β_1	38.80	40.61	67.44	42.4[a]	
	β_2	34.91	38.63	61.04	39.6[a]	
6:0	β_1	33.36	35.67	–		
	β_2	12.95	26.61	–		
8:0	β_1	47.99	50.18	88.42		
	β_2	37.83	42.92	78.39		
10:0	β_1	47.95	53.29	88.62	54.5[c]	
	β_2	44.96	49.36	84.99		
12:0	β_1	58.84	60.96	108.08	~59[d]	
	β_2	53.80	57.30	97.02	56[d]	
14:0	β_1	59.77	61.44	118.91	~66[e]	~64[f]
	β_2	52.31	56.89	78.79		
16:0	β_1	70.04	73.11	129.05	72.0[g]	
	β_2	69.46	71.75	121.32	70.0[g]	
18:1	β_1	42.11	42.83	120.29	46[e]	~44[h]
	β_2	36.51	40.64	112.21		

[a] [8]
[b] [24]
[c] [28]
[d] [27]
[e] [29]
[f] [30]
[g] [9]
[h] 69% pure [31]

Table 2 XRD results for 1,3-acyl-palmitoyl-*rac*-glycerols

FA	Short spacings (Å)				
Experimental values					
2:0	4.38w[a]	4.14vs	3.70w	3.61w[a]	3.56m
4:0	4.57s	3.80s[a]	3.74vs		
6:0	4.62w	3.82vs	3.74m		
8:0	4.56s	3.77s[a]	3.71vs		
10:0	4.60vs	4.48m	3.87m	3.67s	
12:0	4.58vs	3.79s	3.72s		
14:0	4.63vs	4.53m[a]	3.87m	3.67s	
16:0	4.63vs	4.52m[a]	3.73w[b]		
18:1	4.64vs	3.76m	3.67w[a]		
Literature values					
2:0	4.38s	4.14vs	3.54ms		[8]
	4.34w	4.11vs	3.80w	3.54m	[24]
4:0	4.59vs	3.85vs	3.76vs		[8]
12:0	4.63vs	3.8vs	3.76vs		[27]
16:0 by polymorph:					[9]
β_1	4.64vs	4.55s	3.82s	3.74s	
β_2	4.68vs	4.55s	3.90s	3.78s	3.69s

[a] Shoulder
[b] Low-hump

Table 3 FTIR data for carbonyl-stretch absorption band of 1,3-acyl-palmitoyl-*rac*-glycerols in high-melting form

FA	Wavenumber (cm^{-1})	
2:0	–	1,732
4:0	1,707	1,732
6:0	1,709	1,732
8:0	1,709	1,732
10:0	1,713	1,732
12:0	1,709	1,732
14:0	1,715	1,730
16:0	1,709	1,732
18:1	1,707	1,730

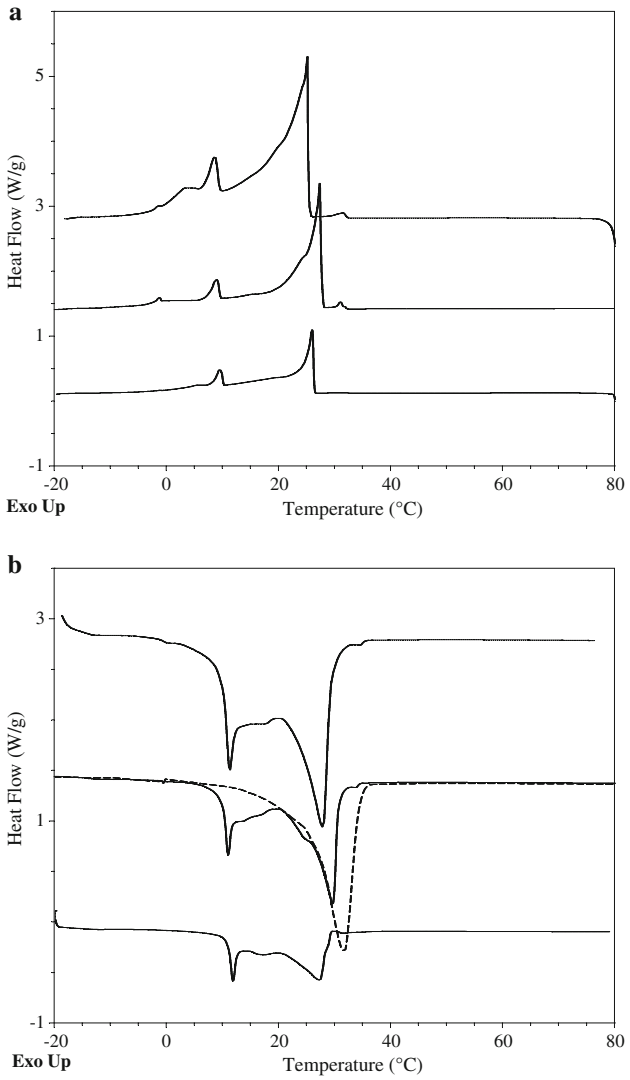

Fig. 1 DSC curves for **a** crystallization and **b** melting of 1,3-acetoyl-palmitoyl-*rac*-glycerol. Plots in each graph were measured at 10 °C/min (*top*), 5 °C/min (*middle*) and 2.5 °C/min (*bottom*). *Dashed line* indicates first melt of high-melting form at 5 °C/min

Results

In the following paragraphs, physical data relating to each of the prepared compounds is detailed. The synthesis, purification and analysis of these compounds, along with NMR results and TLC R_f has been discussed in a prior publication [15]. The most-thermodynamically stable polymorph was obtained by storing each sample at −30 °C for at least 1 week, and was evaluated by DSC, XRD and FTIR (Tables 1, 2 and 3). DSC melting data for the β_1 and β_2 forms (or β' where they occur) is reported for melts at 5 °C/min. Crystallization and melting behavior was collected at 2.5, 5 and 10 °C/min by DSC to detect and evaluate polymorphism—these plots are reproduced here. Finally, SAXS results for all compounds are compared and, based on the observed trends, the molecular arrangement within the unit cell is determined for 1,3-acyl-palmitoyl-*rac*-glycerols.

1,3-Acetoyl-Palmitoyl-*rac*-Glycerol (2:0-OH-16:0)

1,3-Acetoyl-palmitoyl-*rac*-glycerol (2:0-OH-16:0) is a pliable, waxy white solid with texture similar to Parafilm® at room temperature. The product was isolated from the crude product directly by flash chromatography recovering 21.5% yield for a product that is 84.97% pure (by GC). Difficulties encountered while preparing diacid 1,3-DAG of high purity have been discussed in detail previously [15]. The main peaks along with additional peaks due to polymorphism are visible in DSC heating and cooling curves (Fig. 1). The melting point of the β' form ($T_e = 25.33$ and $T_p = 31.55$ °C) and an additional peak ($T_p = 11.8$ °C) were determined by DSC (Table 1). Melting points in the literature for the β' form (43.6 and 41.0 °C) [8, 24] are a great deal higher than this. However, these discrepancies can most likely be attributed to

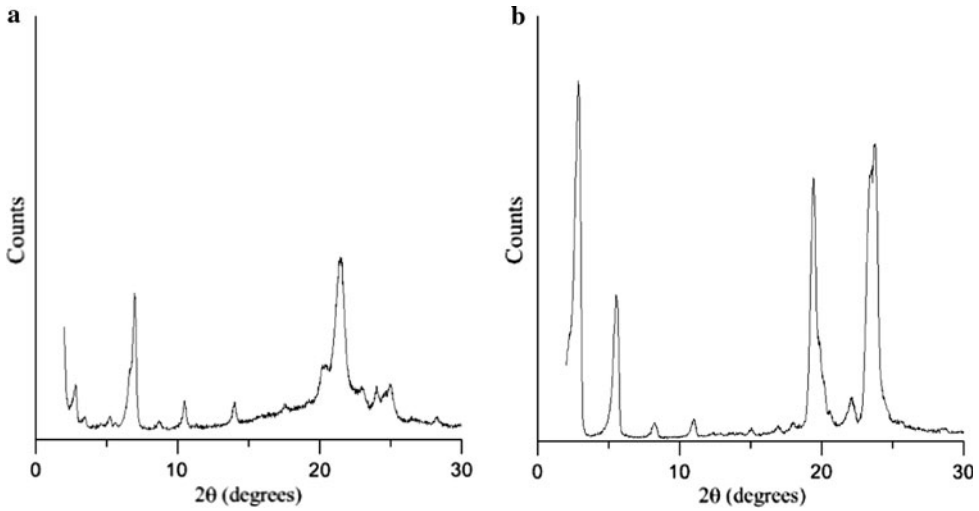

Fig. 2 X-ray powder diffraction results for high-melting forms of: **a** 1,3-acetoyl-palmitoyl-*rac*-glycerol (2:0-OH-16:0) β' form and **b** 1,3-butyroyl-palmitoyl-*rac*-glycerol (4:0-OH-16:0) β_1 form

limitations of preparative and analytical methodologies and to differences in the purity of available starting materials in previous studies. The XRD results for the current study are almost identical to those reported in previous studies for the β' form (Fig. 2; Table 2) [8, 24]. Interestingly, the β' form has only one IR absorption peak in the carbonyl stretching region indicating hydrogen-bonding in the β' form is uniform (Fig. 3; Table 3). In addition, two methylene rocking vibrations (719.5 and 729 cm^{-1}) indicate methylene groups in adjacent acyl chains are packed in an orthorhombic perpendicular arrangement (i.e. β'-form) [25].

1,3-Butyroyl-Palmitoyl-*rac*-Glycerol (4:0-OH-16:0)

1,3-Butyroyl-palmitoyl-*rac*-glycerol (4:0-OH-16:0) is a loose, white, talc-like powder at room temperature. Pure product was isolated by flash chromatography of the crude product with recoveries of 24.0% (yield) for a product that is 92.94% pure (by GC). The main peaks along with an additional peak due to polymorphism are visible in DSC heating and cooling curves (Fig. 4). The melting points of both β_2 and β_1 forms ($T_e = 34.91$ and 38.80 °C correspondingly) were determined by DSC, as was the melting point of the meta-stable form ($T_p = 27.99$ °C) (Table 1). Melting points of 42.4 (form I), 39.6 (form II) and 29.4 °C (form III) have been reported previously for a sample that was approximately 96% pure by both melting point and hydroxyl value [8]. Melting points for forms II and III correspond well with those for β_1 and β_2 in this work, suggesting the reported melting point for form I is actually due to a contaminant. This would not be surprising given the quality of starting materials and analytical methodologies available at the time. The main peaks in the XRD spectra for the β_1 form (4.57, 3.80 and 3.74 Å) are similar to those previously reported (4.59, 3.83 and 3.76 Å) [8] (Fig. 2; Table 2).

1,3-Hexanoyl-Palmitoyl-*rac*-Glycerol (6:0-OH-16:0)

1,3-Hexanoyl-palmitoyl-*rac*-glycerol (6:0-OH-16:0) is a fine white powder that becomes creamy when worked at room temperature. It was isolated from the crude product by flash chromatography with recovery approaching 60% yield for a product that is 86.05% pure (by GC). Purification of prepared diacid 1,3-DAG is confounded by numerous factors as outlined previously [15]. DSC heating and cooling curves were difficult to interpret due to the polymorphic behavior of this compound (Fig. 4). The melting points of both β_2 and β_1 forms ($T_p = 26.61$ and $T_e = 33.36$ °C, correspondingly) were determined by DSC and extensive polymorphism was observed, confounding DSC determination of ΔH_f and T_e for the β_2 form (Fig. 4d; Table 1). The main peaks in the XRD spectra for the β_1 form (4.62, 3.82 and 3.74 Å) are similar to those previously reported (Table 2). A CAS number has yet to be assigned for this compound indicating synthesis and characterization has not been reported previously.

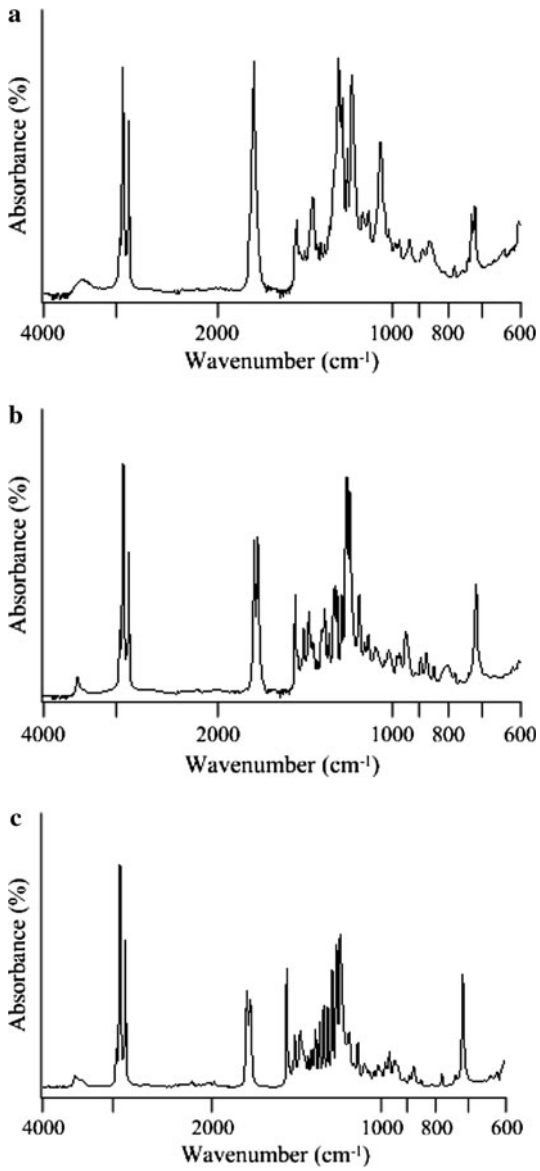

Fig. 3 FTIR for high-melting forms of: **a** 1,3-acetoyl-palmitoyl-*rac*-glycerol (2:0-OH-16:0) β' form; **b** 1,3-hexanoyl-palmitoyl-*rac*-glycerol (6:0-OH-16:0) β_1 form; and **c** 1,3-dipalmitoyl-glycerol (16:0-OH-16:0) β_1 form

1,3-Octanoyl-Palmitoyl-*rac*-Glycerol (8:0-OH-16:0)

1,3-Octanoyl-palmitoyl-*rac*-glycerol (8:0-OH-16:0) is a clean, white waxy solid at room temperature. The pure product (91.63% by GC) was isolated by flash chromatography from a fraction obtained by recrystallization from

acetone (51% yield for recrystallized solid). The use of melt crystallization to isolate 8:0-OH-16:0 from its positional isomers has been disclosed in a patent; however, actual melting point data for this compound has not been reported [26]. The main peaks are visible in DSC heating and cooling curves (Fig. 5). The melting points of both β_2 and β_1 forms (T_e = 37.83 and 47.99 °C correspondingly) were determined by DSC and no extra polymorphs were observed (Table 1). The main peaks in the XRD spectra for the high-melting β_1 form (4.56, 3.77 and 3.71 Å) (Table 2) are similar to those previously reported for the β form of 4:0-OH-16:0 (4.59, 3.83 and 3.76 Å) [8] and the β form of 12:0-OH-16:0 (4.63, 3.80 and 3.76 Å) [27].

1,3-Decanoyl-Palmitoyl-*rac*-Glycerol (10:0-OH-16:0)

1,3-Decanoyl-palmitoyl-*rac*-glycerol (10:0-OH-16:0) is a white solid with a texture similar to bar soap. Product (73.98% by GC) was isolated by flash chromatography from a fraction obtained by recrystallization from acetone (62% yield for recrystallized solid). A number of factors make the isolation of prepared diacid 1,3-DAG difficult as discussed previously [15]. The main peaks along with additional peaks due to polymorphism are visible in DSC heating and cooling curves (Fig. 5). The melting points of both β_2 and β_1 forms (T_e = 44.96 and 47.96 °C correspondingly) were determined by DSC (Table 1). Considering its purity, the β_1 form's T_e is close to the previously reported melting point (determined by Kofler bench) of 54.5 °C (99% purity) [28]. The main peaks in the XRD spectra for the high-melting β form (4.60, 4.48, 3.87 and 3.67 Å) are similar to those of other prepared 1,3-DAG (Table 2).

1,3-Lauroyl-Palmitoyl-*rac*-Glycerol (12:0-OH-16:0)

1,3-Lauroyl-palmitoyl-*rac*-glycerol (12:0-OH-16:0) is a fine, slightly grainy white powder at room temperature. A 45% yield of >99% pure (by GC) product was attained by two successive recrystallizations. The main peaks along

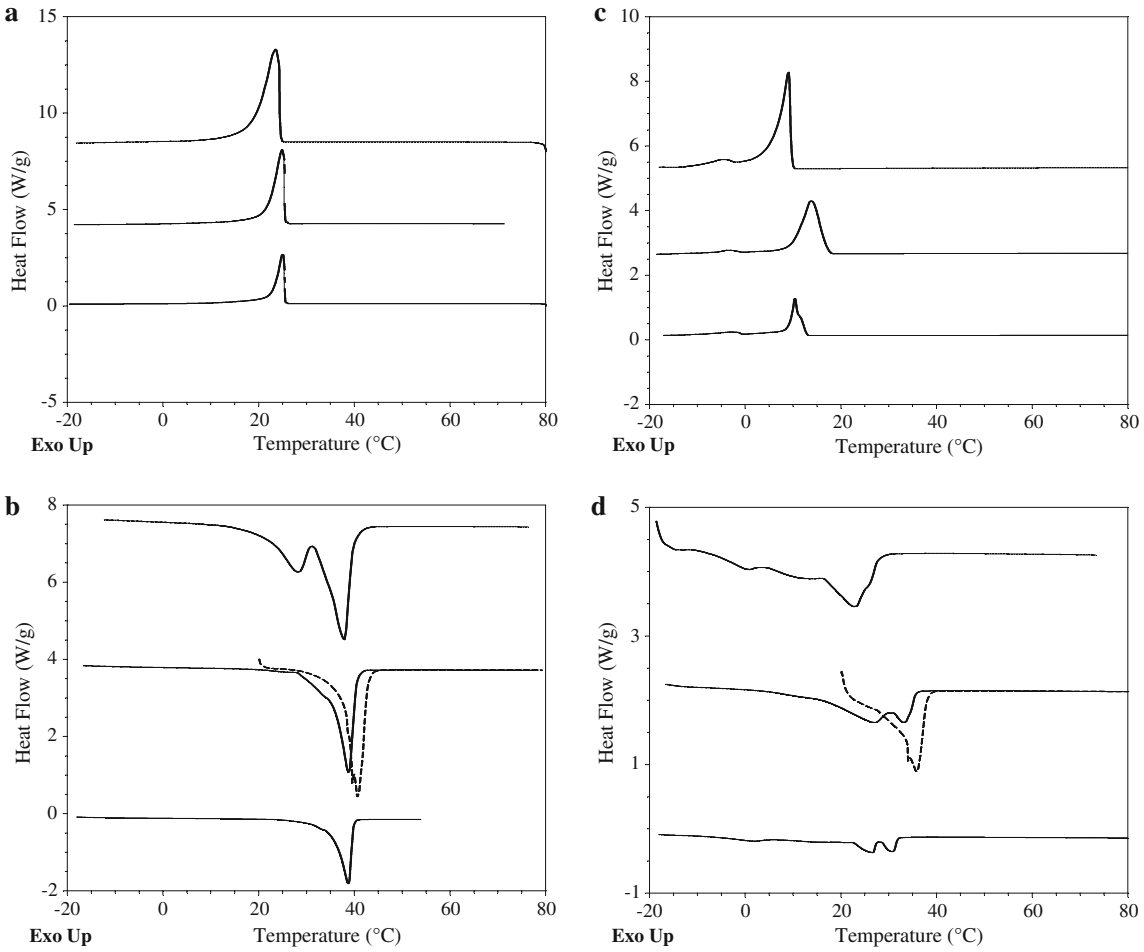

Fig. 4 DSC curves for **a** crystallization and **b** melting of 1,3-butyroyl-palmitoyl-*rac*-glycerol and **c** crystallization and **d** melting of 1,3-hexanoyl-palmitoyl-*rac*-glycerol. Plots in each graph were measured at 10 °C/min (*top*), 5 °C/min (*middle*) and 2.5 °C/min (*bottom*). *Dashed line* indicates first melt of high-melting form at 5 °C/min

with additional peaks due to polymorphism are visible in DSC heating and cooling curves (Fig. 6). The melting points of both β_2 and β_1 forms ($T_e = 53.80$ and 58.84 °C, correspondingly) were determined by DSC (Table 1). This data compares favorably with values reported previously (56 °C for Form II—i.e. β_2 and 59–59.5 °C for Form I—i.e. β_1) [27] (Table 1). The main peaks in the XRD spectra for the β_1 form (4.58, 3.79 and 3.72 Å) are similar to those previously reported (4.63, 3.80 and 3.76 Å) [27] (Table 2).

1,3-Myristoyl-Palmitoyl-*rac*-Glycerol (14:0-OH-16:0)

1,3-Myristoyl-palmitoyl-*rac*-glycerol (14:0-OH-16:0) is a white, slightly grainy solid with a light and fluffy flour-like texture at room temperature. Product (72.62% purity by GC) was purified by two successive recrystallizations. The main peaks are visible in DSC heating and cooling curves (Fig. 6). The melting points of both β_2 and β_1 forms ($T_e = 52.31$ and 59.77 °C, correspondingly) were determined by DSC and no extra peaks due to polymorphism were observed (Table 1). Literature melting points reported for this compound are 65.5–66.5 °C [29] and 63.5–64 °C [30] (Table 1). While these melting points are somewhat in agreement, a purer sample would have had a higher melting point and consequently better agreement. The main peaks in the XRD spectra for the high-melting β form (4.63, 4.53, 3.87 and 3.67 Å) are similar to those reported in the literature for 16:0-OH-16:0 (4.64, 4.55, 3.82 and 3.74 Å) [9] (Table 2).

1,3-Dipalmitoyl-glycerol (16:0-OH-16:0)

1,3-Dipalmitoyl-glycerol (16:0-OH-16:0) is a light and fluffy white powder with a texture similar to flour at room temperature. This product was purified (>99% by GC) by two successive recrystallizations from hexane/ethyl acetate (97:3, v/v) for an overall yield of 35%. The main peaks are visible in DSC heating and cooling curves (Fig. 7). The tops of the exothermic peaks in the crystallization curves are distorted by the melt and subsequent recrystallization of

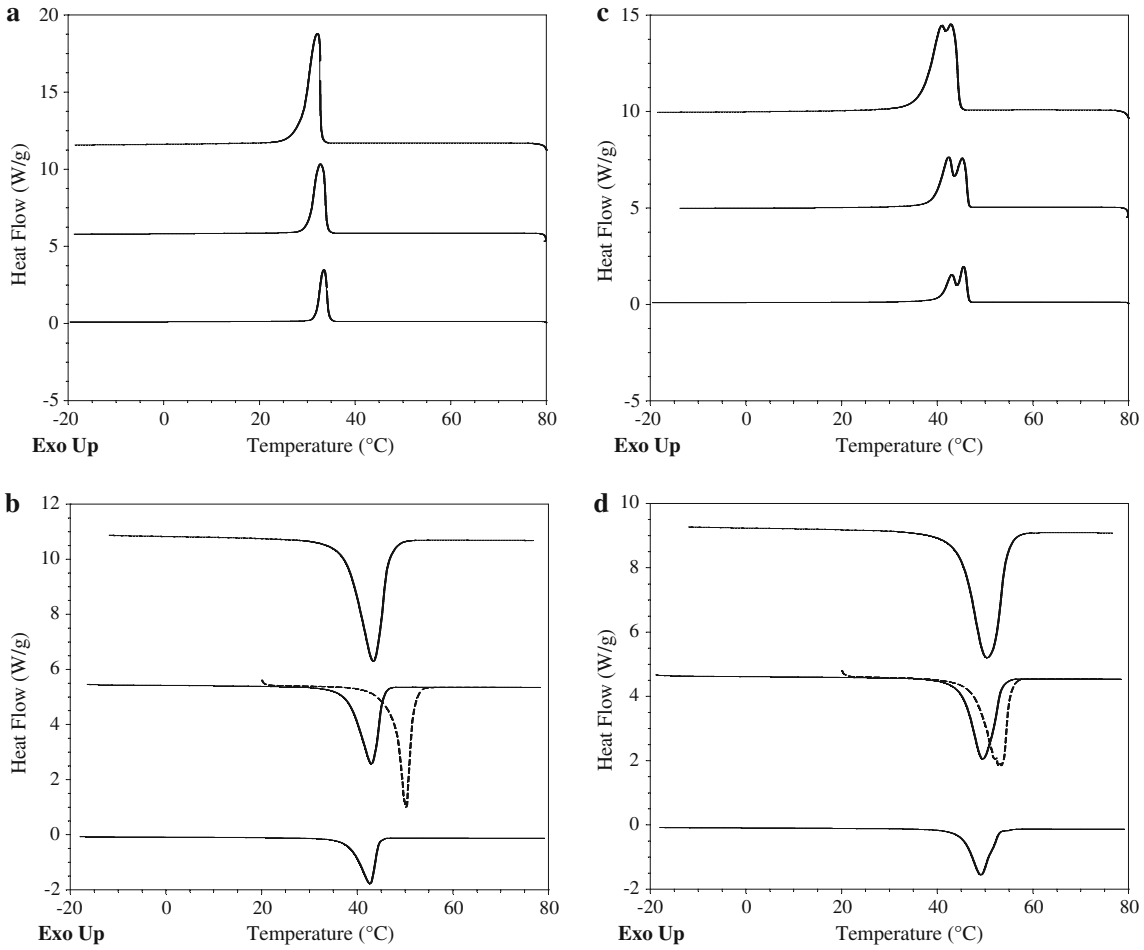

Fig. 5 DSC curves for **a** crystallization and **b** melting of 1,3-octanoyl-palmitoyl-*rac*-glycerol and **c** crystallization and **d** melting of 1,3-decanoyl-palmitoyl-*rac*-glycerol. Plots in each graph were measured at 10 °C/min (*top*), 5 °C/min (*middle*) and 2.5 °C/min (*bottom*). *Dashed line* indicates first melt of high-melting form at 5 °C/min

the sample caused by rapid evolution of heat. The melting points of both β_2 and β_1 forms ($T_e = 69.46$ and 70.04 °C, correspondingly) were determined by DSC and no extra peaks due to polymorphism were observed (Table 1). This melting data agrees with literature values ($T_p = 70$ and 72 °C, correspondingly); however, the enthalpies of fusion ($\Delta H_f = 121.32$ kJ/mol for β_2 and 129.05 kJ/mol for β_1) are larger than in previous reports (109.4 and 113.9 kJ/mol correspondingly) [9] (Table 1). The main peaks in the XRD spectra for the high-melting β form (4.63, 4.52 and 3.73 Å) are similar to those previously reported (4.64, 4.55, 3.82 and 3.74 Å) [9] (Table 2).

1,3-Oleoyl-Palmitoyl-*rac*-Glycerol (16:0-OH-18:1)

1,3-Oleoyl-palmitoyl-*rac*-glycerol (16:0-OH-18:1) is a fine, grainy white powder at room temperature. Pure product (95.22% by GC) was isolated by flash chromatography from a fraction that was obtained by two successive recrystallizations (1st acetone, 2nd hexane/ethanol; 80:20) (46% yield for recrystallized solid). The main peaks are visible in DSC heating and cooling curves (Fig. 7). The melting points of both β_2 and β_1 forms ($T_e = 36.51$ and 42.11 °C correspondingly) were determined by DSC and no extra peaks due to polymorphism were observed (Table 1). This melting point is much lower than those previously reported for the β_1 form: 46 °C [29] and 44–44.5 °C (69% purity) [31]. However, given the relative quality of starting materials and analytical methodologies available in the past, our sample is probably a better representative (95.22% by GC). The main peaks in the XRD spectra for the β_1 form (4.64, 3.76 and 3.67 Å) are similar to those previously reported for other 1,3-DAG (Table 2).

Discussion

The most thermodynamically stable crystal form for 1,3-acyl-palmitoyl-*rac*-glycerols, with one exception, is β_1. The exception, 1,3-acetoyl-palmitoyl-*rac*-glycerol is

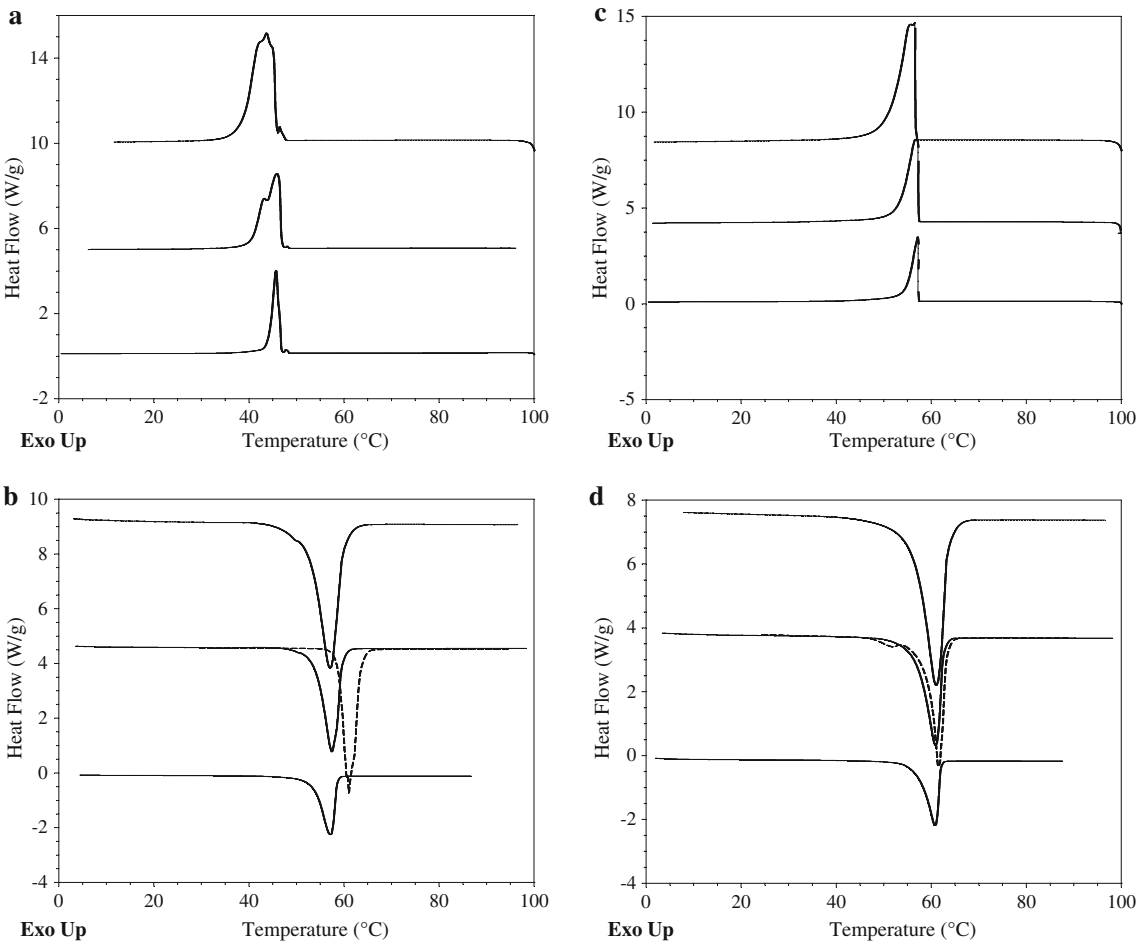

Fig. 6 DSC curves for **a** crystallization and **b** melting of 1,3-lauroyl-palmitoyl-*rac*-glycerol and **c** crystallization and **d** melting 1,3-myristoyl-palmitoyl-*rac*-glycerol. Plots in each graph were measured at 10 °C/min (*top*), 5 °C/min (*middle*) and 2.5 °C/min (*bottom*). *Dashed line* indicates first melt of high-melting form at 5 °C/min

β'-tending. Differences in polymorph were confirmed by both XRD and IR measurement (Figs 2, 3; Tables 2, 3). Meta-stable polymorphs were observed: (1) in the melting curves for three of the prepared 1,3-DAG (i.e. 1,3-acetoyl-, -butyroyl- and -hexanoyl-palmitoyl-*rac*-glycerol); and (2) in the crystallization curves for two of the prepared 1,3-DAG (i.e. 1,3-decanoyl- and -lauroyl-palmitoyl-*rac*-glycerol). For large differences in acyl chain length (case 1 above), the metastable form crystallizes and persists until it is melted—at which point, a more stable polymorph is formed. For smaller differences in acyl chain length (case 2 above), the metastable form crystallizes but does not persist and is not detected in the melting curve. This behavior is a reflection of differences in free energy between meta-stable and stable forms as well as differences in the activation energy between these forms. Interestingly, meta-stable forms occur far more frequently than was originally thought (five of the nine cases presented here).

Melting points for 1,3-acyl-palmitoyl-*rac*-glycerols increased with increasing chain length for saturated FA chains (2:0–16:0) excluding 1,3-hexanoyl-palmitoyl-*rac*-glycerol. Similarly, the hexanoyl derivative in a series of 1,2-dipalmitoyl-3-acyl-sn-glycerols (2:0–16:0) was the lowest melting in the series [32]. The melting behavior in that case, however, was extremely different since the melting points increased as the acyl chain length both increased and decreased from 6:0. This phenomenon was attributed to polymorphic and polytypic differences within the series. In the current case, polymorphic and polytypic behavior (determined by SAXS discussed below) was far more uniform and thus a simpler trend was observed. However, the melting curve of 1,3-hexanoyl-palmitoyl-*rac*-glycerol demonstrated remarkable polymorphism and, considering its relative purity, the melting point determined for the high-melting form may indeed be underestimated.

Experimental results from small angle X-ray scattering measurements on high-melting forms of 1,3-acyl-

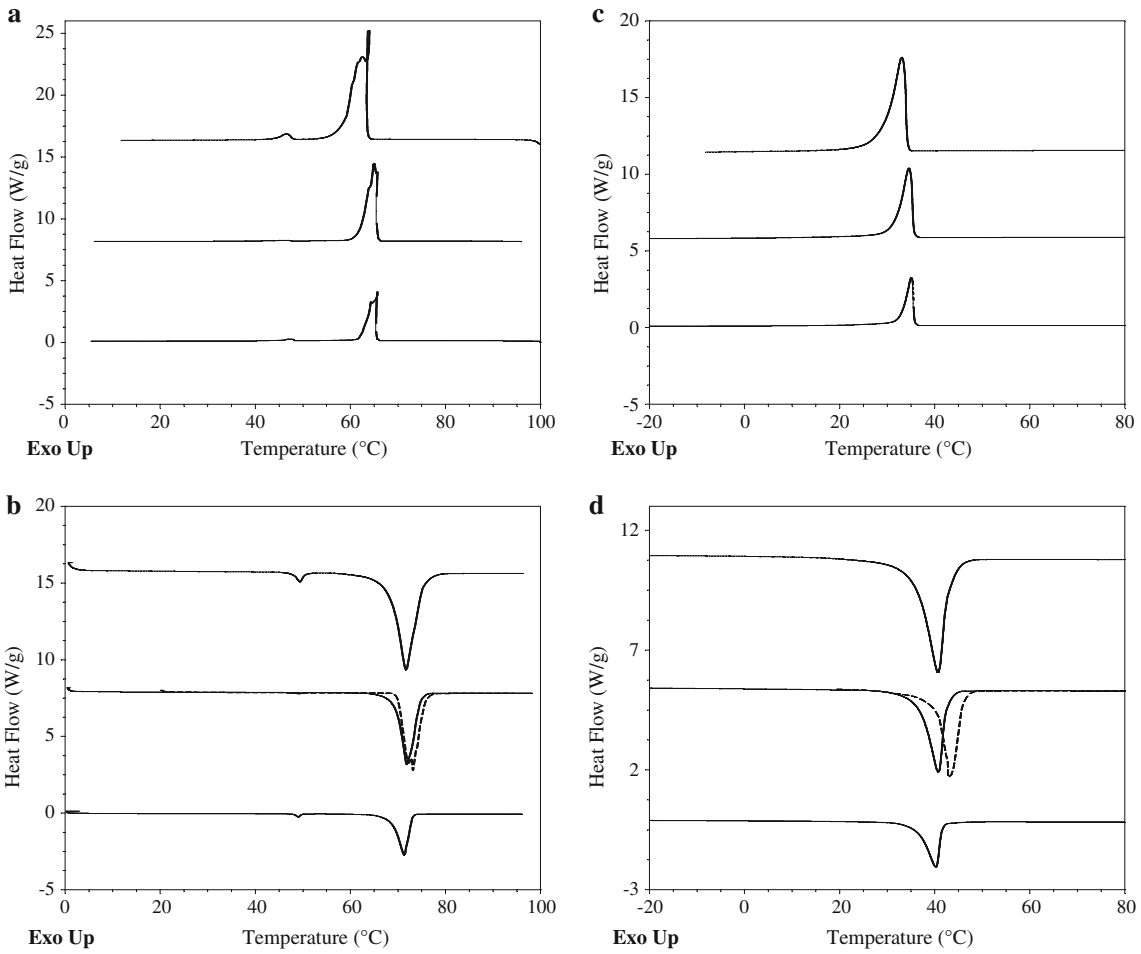

Fig. 7 DSC curves for **a** crystallization and **b** melting of 1,3-dipalmitoyl-glycerol and **c** crystallization and **d** melting 1,3-oleoyl-palmitoyl-*rac*-glycerol. Plots in each graph were measured at 10 °C/min (*top*), 5 °C/min (*middle*) and 2.5 °C/min (*bottom*). *Dashed line* indicates first melt of high-melting form at 5 °C/min

palmitoyl-*rac*-glycerols are listed in Table 4. Also listed are values calculated using the equation:

$$d = 1.268\text{CN} + 7.07 \quad (1)$$

where, d is the long spacing and CN is the carbon number. Equation (1) was derived by linear regression ($R^2 = 0.9998$) using long-spacing data for monoacid 1,3-DAG of 18:0, 16:0, 14:0, 12:0 and 10:0 FA (52.8, 47.5, 42.6, 37.4 and 32.5 Å, respectively) [33]. For the most part, the long spacings of diacid 1,3-DAG determined experimentally were very close to these calculated values (viz. 1,3-butyroyl-, -hexanoyl-, -octanoyl-, -decanoyl- and -lauroyl-palmitoyl-*rac*-glycerols). Indicating acyl chains of the same length associate and regular chain-end matching between terminal methyl groups delineates the lamellae (Fig. 8).

Not all experimentally determined long spacings were well-matched with calculated values (viz. 1,3-acetoyl-, -myristoyl-. -palmitoyl- and -oleoyl-palmitoyl-*rac*-glycerol). Discrepancies are due to differences in structure (oleoyl is *cis* unsaturated, acetoyl is very short-chain), polymorph (1,3-acetoyl-palmitoyl-*rac*-glycerol is β'-stable), tempering or purity. The oleic acid derivative has an experimental long spacing of 45.96 Å which is much less than the calculated value based on saturated monoacid 1,3-DAG (50.17 Å). This is not unexpected since 1,3-DAG with cis unsaturated chains yield smaller long spacings than their saturated counterparts. For example, long spacings for the β_1 forms of 1,3-distearin and 1,3-diolein are 52.8 and 39.3 Å, respectively [33, 34]. Likewise, the acetic acid derivative has an experimental long spacing of 49.85 Å which is much greater than the calculated value (29.89 Å), although a minor peak does occur at 31.07 Å. This indicates the majority of 1,3-acetoyl-palmitoyl-*rac*-glycerol molecules are oriented differently than other diacid 1,3-DAG. Molecules in crystalline 1,3-acetoyl-palmitoyl-*rac*-glycerol appear to be arranged in a manner similar to 1(3)-monopalmitin as suggested by Feuge and Lovegren [8]. Hypothetical addition of the appropriate length for a single or double layer of acetyl chains (2.54 or 5.07 Å, respectively) to the long spacing for 1-monopalmitin (45.8 Å) yields calculated long spacings of either 48.34 or 50.87 Å. Both these values are well within range of the experimental value (49.85 Å) indicating there may be full, partial or no interdigitation of acetoyl chains on adjacent molecules. Furthermore, the aforementioned long spacing is for a 2L polytype and assumes the angle between adjacent 1,3-acetoyl-palmitoyl-*rac*-glycerol molecules will be the same as for adjacent 1(3)-monopalmitin molecules.

Table 4 SAXS results for 1,3-acyl-palmitoyl-*rac*-glycerols

FA	Experimental d (Å)	Calculated[a] d (Å)	Literature d (Å)
2:0	49.85[b]	29.89	41.0[c], 50.46[d]
4:0	32.21	32.42	65.46[d]
6:0	34.74	34.96	
8:0	37.55	37.49	
10:0	39.75	40.03	
12:0	42.63	42.56	42.7[e]
14:0	42.84	45.10	
16:0	45.25	47.63	
18:1	45.96	50.17	

[a] $d = 1.268$ CN + 7.07

[b] Minor peak at 31.07 Å

[c] [24]

[d] [8]

[e] [27]

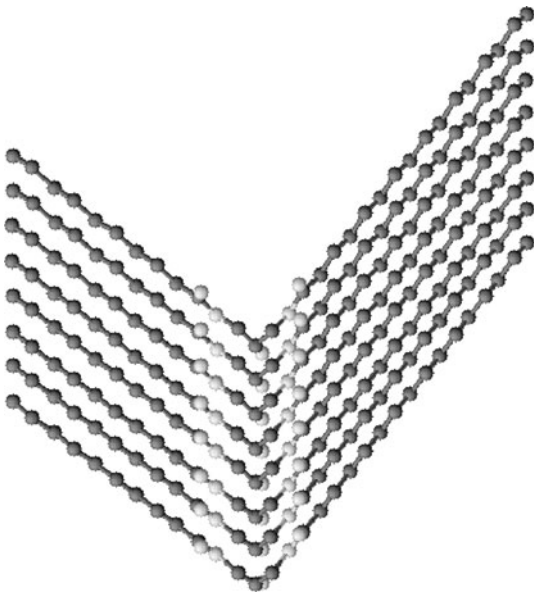

Fig. 8 Orientation of acyl chains in β_1-form of 1,3-decanoyl-palmitoyl-*rac*-glycerol (based on [11]). View down the *a*-axis with *b*- and *c*-axis vertical and horizontal, respectively, along the page

Acknowledgments Financial support for this project was provided by Dairy Farmers of Ontario, Ontario Centres of Excellence and National Sciences and Engineering Research Council of Canada; we are grateful for their generosity. Thanks also to Japan VAM & POVAL Co., Ltd. for their donation of vinyl esters of fatty acids.

References

1. Chawla P, deMan JM (1994) Effect of temperature cycling on the crystalline form, size and textural properties of margarine fats. J Food Lipids 1:313–314
2. Hernqvist L, Herslof B, Larsson K, Podlaha O (1981) Polymorphism of rapeseed oil with a low content of erucic acid and possibilities to stabilize the β'-crystal form in fats. J Sci Food Agric 32:1197–1202
3. Siew W-L, Ng W-L (1999) Influence of diglycerides on crystallization of palm oil. J Sci Food Agric 79:722–726

4. Smith PR, Cebula DJ, Povey MJW (1994) The effect of lauric-based molecules on trilaurin crystallization. J Am Oil Chem Soc 71:1367–1372
5. Xu X, Skands ARH, Adler-Nissen J (2001) Purification of specific structured lipids by distillation: effects on acyl migration. J Am Oil Chem Soc 78:715–718
6. Christophe AB (2005) Structural effects on adsorption, metabolism, and health effects of lipids Inc. In: Shahidi F (ed) Bailey's industrial oil and fat products. John Wiley, Hoboken, pp 535–553
7. Larsson K (1986) Physical properties—structural and physical characteristics. In: Gunstone FD, Harwood JL, Padley FB (eds) The lipid handbook. Chapman and Hall, London, pp 321–384
8. Feuge RO, Lovegren NV (1956) Dilatometric properties of some butyropalmitins, butyrostearins and acetopalmitins. J Am Oil Chem Soc 33:367–371
9. Shannon RJ, Fenerty J, Hamilton RJ, Padley FB (1992) The polymorphism of diglycerides. J Sci Food Agric 60:405–417
10. Gunstone FD, Harwood JL, Dijkstra AJ (2007) The lipid handbook dictionary (CD) in The Lipid Handbook. CRC Press, Boca Raton
11. Hybl A, Dorset D (1971) The crystal structure of the 1,3-diglyceride of 11-bromoundecanoic acid. Acta Crystallogr A B27:977–986
12. Larsson K (1963) The Crystal Structure of the 1,3-diglyceride of 3-thiadodecanoic acid. Acta Crystallogr A 16:741–748
13. Nutter B (2009) Nu-Chek Prep, Inc. Catalog 2009/2010, Elysian
14. Gaffney PRJ, Reese CB (2001) Synthesis of naturally occurring phosphatidylinositol 3, 4, 5-triphosphate [PtdIns(3, 4, 5)P3] and its diastereomers. J Chem Soc Perkin Trans 1:192–205
15. Craven RJ, Lencki RW (2010) Preparation of diacid 1,3-diacylglycerols. J Am Oil Chem Soc 87(11):1281–1291
16. Halldorsson A, Magnusson CD, Haraldsson GG (2003) Chemoenzymatic synthesis of structured triacylglycerols by highly regioselective acylation. Tetrahedron 59:9101–9109
17. Quinn JG, Sampugna J, Jensen RG (1967) Synthesis of 100-gram quantities of highly purified mixed acid triglycerides. J Am Oil Chem Soc 44:439–442
18. Jensen RG, Pitas RE (1976) Synthesis of some acylglycerols and phosphoglycerides. In: Paoletti R, Kritchevsky D (eds) Advances in Lipid Research. Academic Press, New York, pp 214–247
19. Yu CC, Lee Y-S, Cheon BS, Lee SH (2003) Synthesis of glycerol monostearate with high purity. Bull Korean Chem Soc 24: 1229–1231
20. Bernstein J (2002) Polymorphism in molecular crystals. Oxford University Press, Oxford
21. Hohne GWH, Hemminger WF, Flammersheim HJ (2003) Differential scanning calorimetry. Springer, New York
22. Laye PG (2002) Differential thermal analysis and differential scanning calorimetry. In: Haines PJ (ed) Principles of thermal analysis, calorimetry. Royal Society of Chemistry, Cambridge, pp 55–93
23. Cullity BD (1978) Elements of X-ray diffraction. Addison-Wesley, Reading
24. Martin JB, Lutton ES (1972) Preparation and phase behavior of acetyl monoglycerides. J Am Oil Chem Soc 49:683–687
25. Chapman D (1965) The structure of lipids by spectroscopic and X-ray techniques: with a chapter on separation techniques including thin layer and gas liquid chromatography. Methuen, London
26. De Groot WTM (1972) 1,3-diglycerides by isomerization of 1,2-diglycerides. West Germany Patent: 2156091
27. Sidhu SS, Daubert BF (1946) X-ray investigation of glycerides vs. diffraction analyses of synthetic diacid diglycerides. J Am Chem Soc 68:2603–2605
28. Mank APJ, Ward JP, van Dorp DA (1976) A versatile flexible synthesis of 1,3-diglycerides and triglycerides. Chem Phys Lipids 16(2):107–114
29. Daubert BF, Longenecker HE (1944) Unsaturated synthetic glycerides III. Unsaturated symmetrical mixed diglycerides. J Am Chem Soc 66:53–55
30. Verkade PE, van der Lee J, Meerburg W (1937) The synthesis of glycerides with the help of trityl compounds III. Triacid glycerides (in German). Recueil des Travaux Chemique des Pays-Bas 56:365–374
31. Hartman L (1957) Glyceride synthesis by direct esterification. J Chem Soc 3572–3575
32. Kodali DR, Atkinson D, Redgrave TG, Small DM (1984) Synthesis and polymorphism of 1,2-dipalmitoyl-3-acyl-*sn*-glycerols. J Am Oil Chem Soc 61:1078–1084
33. Howe RJ, Malkin T (1951) An X-ray and thermal examination of the glycerides. Part XI. The 1:2-diglycerides, and further observations on 1:3-diglycerides. J Chem Soc 2663–2667
34. Daubert BF, Lutton ES (1947) X-ray diffraction analyses of synthetic unsaturated monoacid diglycerides. J Am Chem Soc 69:1449–1451